Available online at www.sciencedirect.com
SCIENCE DIRECT®
Bioorganic & Medicinal Chemistry
Bioorganic & Medicinal Chemistry 13 (2005) 1633–1640

Synthesis and cellular studies of an octa-anionic 5,10,15,20-tetra[3,5-(*nido*-carboranylmethyl)phenyl]porphyrin (H_2OCP) for application in BNCT

Vijay Gottumukkala, Raymond Luguya, Frank R. Fronczek and M. Graça H. Vicente*

Department of Chemistry, Louisiana State University, Baton Rouge, LA 70803, USA

Received 8 October 2004; revised 8 December 2004; accepted 8 December 2004
Available online 11 January 2005

Abstract—The total synthesis of 5,10,15,20-tetra[3,5-(carboranylmethyl)phenyl]porphyrins **2**–**5** containing 36–43% boron by weight are reported. All compounds were characterized by spectroscopic methods and, in the case of **2**, by X-ray crystallography. The water-soluble *nido*-carboranylporphyrin **5** (H_2OCP) was found to have low dark toxicity toward V79 lung fibroblasts ($CS_{50} \geqslant 250$ μM), to be readily taken up by human glioblastoma T98G cells in culture and to localize subcellularly preferentially in the cell lysosomes. In comparison with a known tetra(*nido*-carboranyl)porphyrin (**6**), H_2OCP (**5**) is taken up slower and to a lower extent by T98G cells, possibly as a result of its higher hydrophilic character. The metal-free H_2OCP (**5**) was also found to accumulate to a higher extent in T98G cells compared with its zinc(II) complex analog **4**. Our studies show that carboranylporphyrins bearing eight *nido*-carborane cages can still accumulate intracellularly and have low dark toxicity toward cells in culture, and therefore might have promise for application in BNCT.

1. Introduction

Boron neutron capture therapy (BNCT) is a binary therapy for the treatment of high-grade gliomas and metastatic brain tumors, currently undergoing clinical trials in the US, Europe, and Japan.[1–4] In BNCT ^{10}B-rich tumors are irradiated with low-energy neutrons, producing high linear energy transfer particles, $^4He^{2+}$ and $^7Li^{3+}$, which cause irreversible damage to tumor cells. These charged particles have limited ranges in tissue of about one cell diameter therefore the destructive effect is localized to the ^{10}B-containing tumor.[5,6] For successful BNCT, 15–30 μg of ^{10}B/g of tumor must be selectively delivered to tumor tissue; a lower amount of boron-10 is necessary to sustain a lethal $^{10}B(n,\alpha)^7Li$ capture reaction if the boron atoms localize intracellularly, in close proximity to the cell nucleus.[7,8] The only two boron delivery drugs currently used clinically are disodium mercapto-*closo*-dodecaborane (BSH) and L-4-dihydroxyborylphenylalanine (BPA). Both these agents have been found to have low toxicity, moderate selectivity for gliomas and low retention times in tumors. Considerable higher therapeutic efficacy could be achieved in BNCT with the discovery of new ^{10}B-carriers of high boron content, capable of selectively delivering high amounts of boron to tumor cells with low toxicity.[9] Porphyrins have emerged as promising BNCT agents, because of their known selectivity for tumor cells and easy synthesis with high boron content.[10,11] Porphyrin macrocyles containing up to 4 boron clusters (22–32% boron by weight) attached to the porphyrin macrocycle via ester, amide, ether, and carbon–carbon bonds have been synthesized and evaluated in cellular and animal studies. The results from these investigations show that this type of compound can selectively deliver therapeutic concentrations of boron to tumor cells with low toxicity.[10–14] The synthesis of one porphyrin derivative bearing eight boron cages linked to the porphyrin ring via ester bonds has been reported[15] but no studies of its biological properties were undertaken. We report herein the synthesis of boron-containing porphyrins with eight carborane cages (36–43% boron by weight) linked to the porphyrin macrocycle via chemically stable carbon–carbon bonds. We also describe our results from cellular studies using the water-soluble octacarboranylporphyrin **5** and compare them with those found for the zinc(II) complex **4** and for a known tetracarboranylporphyrin (**6**).[16]

Keywords: BNCT; *nido*-Carborane; Carboranylporphyrin; Cytotoxicity; Cellular uptake.
* Corresponding author. Tel.: +1 225 578 7405; fax: +1 225 578 3458; e-mail: vicente@lsu.edu

0968-0896/$ - see front matter © 2004 Elsevier Ltd. All rights reserved.
doi:10.1016/j.bmc.2004.12.016

2. Results

2.1. Porphyrin syntheses

Porphyrins **2**–**5**, containing eight carborane cages linked via carbon–carbon bonds to the *meso*-phenyl groups of the porphyrin ring, were prepared according to Scheme 1. The key intermediate dicarboranylbenzaldehyde **1** was prepared in three steps from commercially available 3,5-dimethylbromobenzene, as we have previously reported.[14,17] The condensation of benzaldehyde **1** with pyrrole using trifluoroacetic acid (TFA) as catalyst followed by oxidation of the porphyrinogen intermediate with *p*-chloranil gave porphyrin **2** in 15% yield. Porphyrin **2** has high hydrophobic character and it is soluble in nonpolar organic solvents, such as carbon tetrachloride and toluene. Addition of one drop of acid, such as TFA, increases the solubility of **2** in chloroform and dichloromethane, via formation of the porphyrin dication. In fact, porphyrin **2** was found to protonate readily, possibly due to the inductive effect of the carborane cages.[18] The conversion of porphyrin **2** into the water-soluble octa-anionic porphyrins **4** and **5** was performed under mild conditions, using a 3:1 mixture of pyridine/piperidine, at room temperature.[14,16] The base-induced deboronation reaction gave a quantitative yield of the corresponding octa(*nido*-carboranyl)porphyrin when performed on the zinc(II) complex **3**, rather than on the free base **2**, and demetallation of porphyrin **4** to give **5** occurred smoothly under acidic conditions. The octasodium salts **4** and **5** were obtained by cation exchange using a Dowex resin in the sodium form. Both octa(*nido*-carboranyl)porphyrins **4** and **5** are highly soluble in polar solvents such as in acetone, methanol, DMSO, and water.

2.2. Molecular structure

Crystals of porphyrin **2** were grown by slow diffusion of cyclohexane into a concentrated solution of **2** in dichloromethane. The molecular structure of porphyrin **2** is shown in Figure 1. The compound crystallized on an inversion center, as a solvate with five cyclohexane molecules and two dichloromethane molecules. One of the cyclohexane molecules also lies on a center. The 24-atom porphyrin core of the molecule is essentially planar, with mean deviation 0.012 Å and maximum 0.019(7) Å. The phenyl rings are nearly orthogonal to the porphyrin plane, forming dihedral angles of 85.5(2) and 89.0(2)° with it, and essentially orthogonal to each other, with a dihedral angle of 89.7(2)°. The carborane cages are all turned in the same direction with respect to the local fourfold axis of the molecule, so that the overall symmetry of the molecule is roughly C_{4h}. Figure 1b shows the molecule viewed slightly oblique to the approximate mirror plane.

2.3. Dark cytotoxicity

The dark toxicity of H_2OCP (**5**) toward V79 hamster fibroblast cells was evaluated using a clonogenic assay, as we have previously reported.[19] Concentrations of H_2OCP (**5**) up to 250 μM and 24-h incubation time were used in this assay. The results obtained are shown in

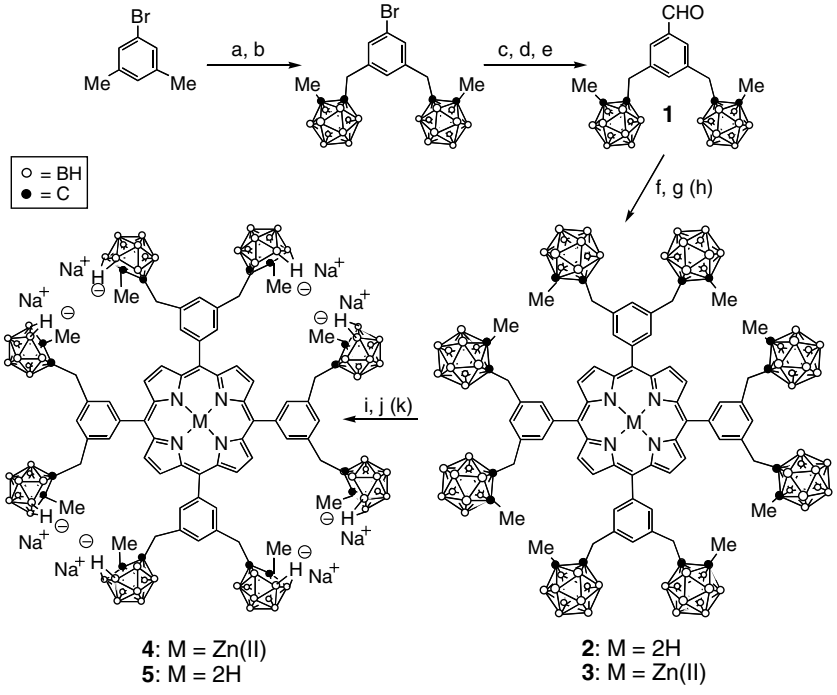

Scheme 1. (a) N-bromosuccinimide, benzoyl peroxide, 16 h reflux in CCl_4 (33%); (b) 1-lithium-2-methyl-*o*-carborane, THF, LiI, room temperature 16 h (63%); (c) *n*-BuLi, THF, −78 °C for 30 min; (d) DMF, −78 °C for 30 min then 0 °C for 1 h; (e) 5% aqueous HCl, room temperature for 15 min (71%); (f) pyrrole, TFA, CH_2Cl_2, room temperature overnight; (g) *p*-chloranil, room temperature for 6 h (15%); (h) $ZnCl_2$, THF/CH_2Cl_2 (1:10), pyridine (50%); (i) pyridine/piperidine (3:1), room temperature for 72 h; (j) Dowex 50WX2-100 in Na^+ form (quantitative); (k) TFA, H_2SO_4, 30 min at room temperature (96%).

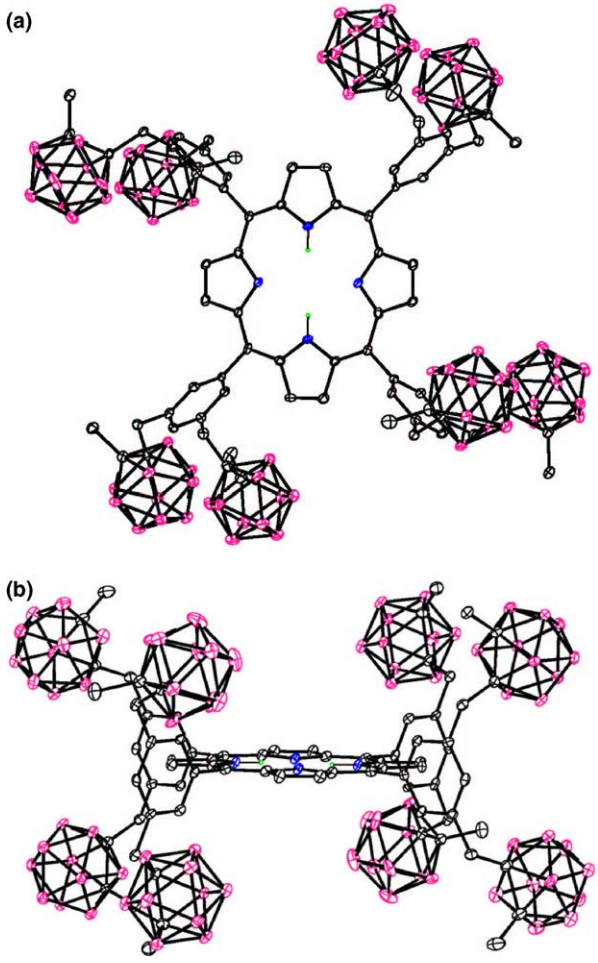

Figure 1. The molecular structure of porphyrin **2** as determined by X-ray crystallography. (a) Top view; (b) side view. Solvent molecules and H atoms, except for N–H, are not shown.

Figure 2. Porphyrin concentrations up to 200 μM had no significant effect on the rate of colony survival, but a decrease in the number of colonies was clearly observed at the higher concentration studied. The 50% colony survival was estimated from Figure 2 to be $CS_{50} \geqslant 250$ μM.

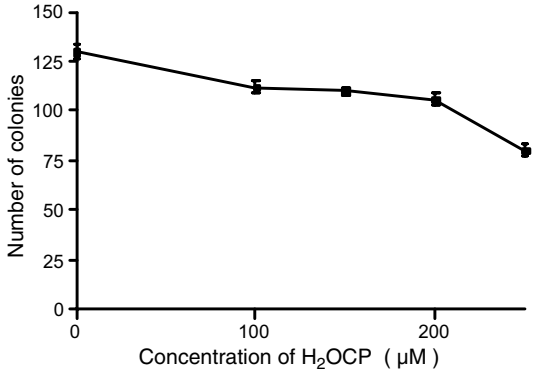

Figure 2. Cytotoxicity of H_2OCP (**5**) toward V79 cells using a clonogenic assay.

2.4. Cellular uptake

The concentration-dependent uptake of H_2OCP (**5**) by human T98G cells was investigated using concentrations up to 200 μM for a period of 3 h. The results obtained are shown in Figure 3. The uptake of H_2OCP (**5**) systematically increased with the concentration of exogenous porphyrin.

The time-dependent uptake of H_2OCP (**5**), its zinc(II) derivative **4** and of the known tetra(*nido*-carboranyl)porphyrin **6** by T98G cells was also studied and the results obtained are shown in Figure 4. All porphyrins were evaluated under the same conditions, at a concentration of 10 μM. The amounts of all porphyrins accumulated in cells increased rapidly with time in the first four hours, although the amount of each porphyrin determined at each time point differed considerably. For the metal-free porphyrins **5** and **6**, the amount taken up by T98G cells reached a plateau after 4 h, whereas for the zinc(II) complex **4** increasing amounts of porphyrin were consistently found over the 24 h uptake time period examined in this study. The tetra(*nido*-carboranyl)porphyrin **6** (Fig. 5) was found to be taken-up to a significantly higher extent by T98G cells compared with the octa(*nido*-carboranyl)porphyrins **4** and **5**.

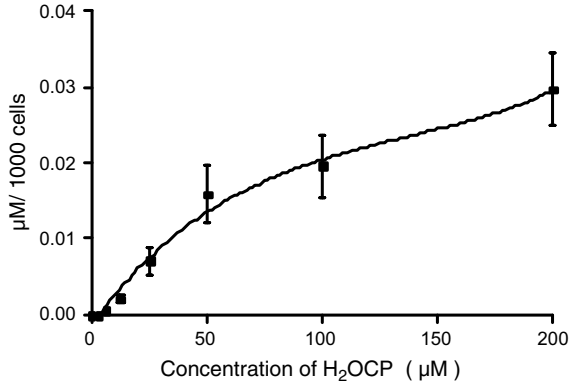

Figure 3. Concentration-dependent uptake of H_2OCP (**5**) by T98G cells, after a 3 h time period.

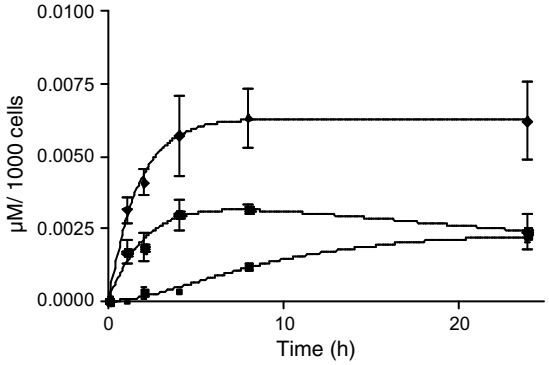

Figure 4. Time-dependent uptake of H_2OCP (**5**) (circles), ZnOCP (**4**) (squares) and porphyrin **6** (diamonds) at 10 μM by T98G cells.

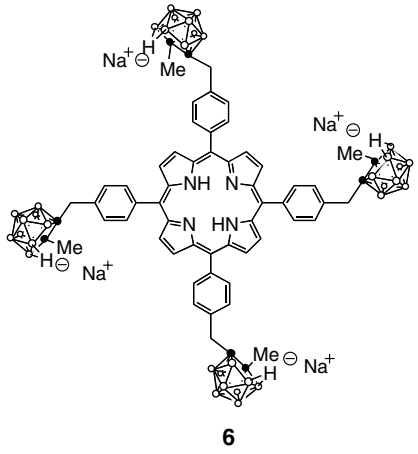

6

Figure 5. Structure of tetra(*nido*-carboranyl)porphyrin **6**.

2.5. Intracellular localization

To evaluate the preferential sites of localization of H_2OCP (**5**) in T98G cells, the cells were exposed to 50 μM concentration of porphyrin **5** for 4 h followed by fluorescence microscopy. As shown in Figure 6B, the intracellular fluorescence has a punctate pattern, suggesting the cell lysosomes as the preferential sites of localization for H_2OCP (**5**). To confirm this hypothesis, a co-localization experiment was performed using the lysosome-specific probe lysoSensor, as shown in Figure 6C and D. The overlay between the porphyrin fluorescence and that of lysoSensor indicates that the two compounds are localized in the same organelle.

3. Discussion

Several boron-containing porphyrins have been synthesized and proposed as delivery agents for the BNCT of tumors.[10,11] Most of these compounds contain 2 or 4 carborane cages linked to the porphyrin macrocycle via ester, ether, amide or carbon–carbon bonds. The nature of this linkage influences their stability and possibly their systemic toxicity. We have recently reported expeditious synthetic routes to carboranylporphyrins bearing hydrolytically stable carbon–carbon bonds.[14,16,17,19,20] The evaluation of both *closo*- and *nido*-carboranylporphyrins in cellular and animal studies has shown that the porphyrin macrocycle is an excellent platform for the selective delivery of boron to tumor cells. Since high amounts of boron are needed for effective BNCT (15–30 μg/g tumor), porphyrins of high boron content are potentially promising delivery vehicles for this therapy. The octa-carboranylporphyrins **2**–**5** were synthesized in moderate yields as shown in Scheme 1. While the *closo*-carboranylporphyrins **2** and **3** are highly hydrophobic and completely insoluble in water, the octa-anionic *nido* analogs **4** and **5** show good solubility in polar solvents (e.g., water, methanol, DMSO) due to their amphiphilic nature. The molecular structure of porphyrin **2** (Fig. 1) exhibits a planar conformation with the *meso*-phenyl rings orthogonal to each other and to the porphyrin plane. In contradistinction, the molecular structures of the Zn(II) complexes of carboranylporphyrins have shown nonplanar waved[21] or saddle[19] conformations, as previously reported. We have also obtained crystals of porphyrin **2** as the dication (dichloride and dipicrate salts) and of zinc(II) complex **3**, but lower resolution structures were obtained from these crystals.[22]

Porphyrin **5** was found to have low dark toxicity toward V79 hamster fibroblast cells using a clonogenic assay ($CS_{50} \geqslant 250$ μM). This result is in agreement with cytotoxicity studies reported in the literature for this type of compound, bearing up to four carborane cages.[19,23,24] Our result indicates, for the first time, that a porphyrin derivative bearing eight *nido*-carborane groups linked to the porphyrin platform via carbon–carbon bonds shows

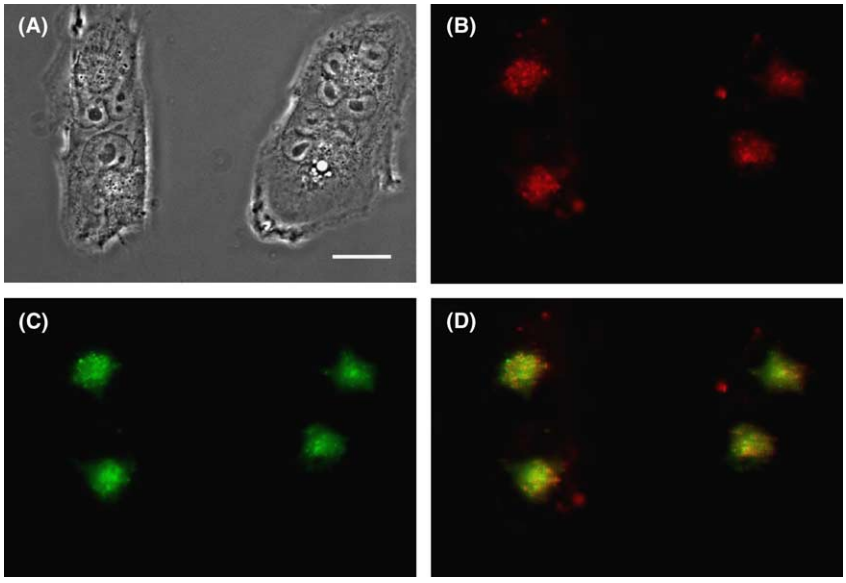

Figure 6. Intracellular localization of H_2OCP (**5**) in T98G cells. A: phase contrast; B: porphyrin fluorescence; C: lysoSensor fluorescence; D: overlay. Scale bar: 20 μm.

similar low dark toxicity to that found for related carboranylporphyrins of lower boron content.

The uptake of carboranylporphyrin **5** in human glioblastoma T98G cells was found to be concentration dependent (Fig. 3), in agreement with the literature.[16] At the lower concentrations tested (up to 50 μM) this dependence was found to be linear, however at the highest concentrations (100 and 200 μM) the amount of porphyrin accumulated was lower than could be expected due to saturation and possibly to residual cytotoxic effects. The accumulation of H_2OCP (**5**) in T98G cells was also time dependent (Fig. 4), as previously reported for this type of compound.[16,23,25] The octa-anionic porphyrins **4** and **5** were accumulated in human T98G cells to a significant lower extent than the tetra-anionic porphyrin **6**, probably due to the higher hydrophilicity of porphyrins **4** and **5** compared with **6**. It is interesting to note that the kinetics of uptake of the two metal-free porphyrins **5** and **6** are very similar (Fig. 4). On the other hand, the Zn(II) complex **4** was taken up at a much slower rate than the metal free porphyrins **5** and **6**. However, after 24 h incubation time the amounts of Zn(II) complex **4** and its metal-free porphyrin **5** found in cells were very similar. These results suggest different mechanisms of uptake of octa-carboranylporphyrins **4** and **5** into tumor cells, probably as a result of their distinct aggregation behavior[18] and isomer composition.[26] Even though the uptake of octa-carboranylporphyrins **4** and **5** was only approximately half that of tetra-carboranylporphyrin **6**, the high boron content porphyrins can potentially deliver therapeutic amounts of boron to tumors with low systemic toxicity, because of their significantly greater boron content. Furthermore, upon activation with low-energy neutrons, the more hydrophilic octa-anionic porphyrins could possibly induce damage to the tumor vasculature in addition to the tumor cells.[27]

The preferential sites of localization of H_2OCP (**5**) within human T98G cells were found to be the cell lysosomes (Fig. 6), in agreement with reported studies on this type of compound.[16,28,29] Negatively charged porphyrins are often observed to localize subcellularly in the lysosomes, which have a low internal pH, possibly as a result of an endocytic mechanism of uptake.[27] The tetra-anionic porphyrin **6** has also been observed to localize preferentially in the cell lysosomes.[16]

4. Conclusions

Carboranylporphyrins of high boron content are promising sensitizers for application in the BNCT treatment of tumors. The water-soluble octa-carboranylporphyrin **5** displays low dark toxicity toward V79 hamster fibroblast cells ($CS_{50} \geqslant 250$ μM) using a clonogenic assay, as previously observed for carboranylporphyrins of lower boron content. Similarly to tetra-carboranylporphyrins, the cellular uptake of H_2OCP (**5**) is both concentration- and time-dependent. The octa-anionic porphyrins **4** and **5** are accumulated in human glioblastoma T98G cells to a significant lower extent than the tetra-anionic porphyrin **6**, probably as a result of their higher hydrophilicity. The time-dependent cellular uptake of the metal-free porphyrins **5** and **6** follows a similar profile, while the Zn(II) complex **4** accumulates at a slower rate over time. The metal free H_2OCP (**5**) accumulates faster and to a higher extent in T98G cells than its Zn(II) derivative **4** at short time periods (up to 8 h), although similar amounts of **4** and **5** were found after 24 h, demonstrating different uptake kinetics for these two porphyrins. The preferential sites of subcellular localization of H_2OCP (**5**) in human glioblastoma T98G cells are the cell lysosomes, possibly as a result of its anionic nature and/or endocytic uptake.

5. Experimental

5.1. Chemistry

All reactions were carried out under an argon atmosphere in dried solvents. Commercially available starting compounds were purchased from Sigma–Aldrich and used directly without further purification. Silica gel 60 (70–230 mesh, Merck) was used for column chromatography. Analytical thin-layer chromatography (TLC) was performed using Merck 60 F254 silica gel (precoated sheets, 0.2 mm thick). ^{1}H NMR spectra were obtained using a Bruker DPX 250 MHz spectrometer; chemical shifts are expressed in ppm relative to TMS (0 ppm). Electronic absorption spectra were measured on a Perkin–Elmer Lambda 35 UV–vis spectrophotometer and fluorescence spectra were measured on a Perkin–Elmer LS55 spectrometer. Mass spectra were obtained on a Bruker Prolix III MALDI-TOF mass spectrometer. Melting points were measured on a MELT-TEMP apparatus.

5.2. Bis[3,5-(1-methyl-*o*-carboranyl)methyl]benzaldehyde (1)

The title compound was prepared according to the literature method,[14] following the synthetic route shown in Scheme 1, mp = 205–207 °C. MS (MALDI) *m/z* 446.4 [M^+]. Anal. Calcd for $C_{15}H_{34}B_{20}O$: C, 40.34; H, 7.67. Found: C, 40.38; H, 7.67. ^{1}H NMR ($CDCl_3$) δ ppm: 1.5–3.0 (br, 20H, BH), 2.20 (s, 6H, CH_3), 3.55 (s, 4H, CH_2), 7.30 (d, 1H), 7.68 (d, 2H), 10.04 (s, 1H, CHO).

5.3. *meso*-Tetra[bis-3,5-(1-methyl-*o*-carboranyl)methylphenyl]porphyrin (2)

A solution of aldehyde **1** (0.243 g, 0.54 mmol) and freshly distilled pyrrole (0.050 mL, 0.72 mmol) in dry dichloromethane (55 mL) was purged with argon for 15 min. TFA (0.03 mL, 0.377 mmol) was added and the final solution was stirred at room temperature overnight (until complete disappearance of the starting aldehyde). After oxidation with *p*-chloranil (0.102 g, 0.41 mmol) for 6 h at room temperature, the final reaction mixture was washed once with an aqueous saturated solution of $NaHCO_3$ and once with water, before being dried over anhydrous Na_2SO_4. After evaporation of the solvent under vacuum, the residue was

purified by column chromatography using 1:2 dichloromethane/petroleum ether for elution. The porphyrin fraction obtained was recrystallized from dichloromethane/methanol, to give 0.16 g (15% yield) of the title compound, mp > 300 °C. MS (MALDI) *m/z* 1977.3. ^{1}H NMR (d-TFA/$CDCl_3$) δ ppm: −0.80 (br, NH), 1.5–3.1 (br, 80H, BH), 2.31 (s, 24H, CH_3), 3.91 (s, 16H, CH_2), 7.72 (s, 4H), 8.33 (s, 8H), 8.74 (s, 8H, β-H). UV–vis ($CHCl_3$) λ_{max}: 419 nm (ε 497,300), 509 (20,250), 543 (8300), 588 (6150), 642 (4300).

5.4. Zinc(II)-*meso*-tetra[bis-3,5-(1-methyl-*o*-carboranyl)methylphenyl]porphyrin (3)

A solution of porphyrin **2** (0.089 g, 0.20 mmol) and zinc(II) chloride (0.400 g) in THF (10 mL) and dichloromethane (100 mL) was stirred at room temperature for 3 h. The solvent was removed under vacuum and the reaction mixture was purified on a short silica gel column, using 2:3 dichloromethane/petroleum ether for elution. The title compound (0.050 g) was obtained in 50% yield, mp > 300 °C. HRMS (MALDI) *m/z* 2040.1766. ^{1}H NMR ($CDCl_3$) δ ppm: 1.6–2.9 (br, 80H, BH), 2.20 (s, 24H, CH_3), 3.75 (s, 16H, CH_2), 7.43 (s, 4H), 8.01 (s, 8H), 8.85 (s, 8H, β-H). UV–vis (CH_2Cl_2) λ_{max}: 419 nm (ε 417,000), 547 (17,200), 582 (3200).

5.5. Zinc(II)-*meso*-tetra[bis-3,5-(1-methyl-*nido*-carboranyl)methylphenyl]porphyrin tetrasodium salt (4)

Porphyrin **3** (0.050 g,0.0245 mmol) was dissolved in a 3:1 mixture of pyridine and piperidine (4.0 mL), and stirred at room temperature in the dark for 72 h, under argon. The solvent was completely removed under vacuum, the residue re-dissolved in a 40% aqueous acetone solution and passed through a Dowex 50WX2-100 resin in the sodium form. The porphyrin fraction was collected, dried under vacuum, redissolved in a 70% aqueous acetone solution and again passed through the ion-exchange resin. After removal of the solvent under vacuum, the anionic porphyrin was obtained as a crystalline solid in quantitative yield, mp > 300 °C. ^{1}H NMR (acetone-d_6) δ ppm: −2.42 (br, 8H, BH) 1.6–2.9 (br, 72H, BH), 2.00 (s, 24H, CH_3), 3.46 (s, 16H, CH_2), 7.86 (s, 4H), 8.06 (s, 8H), 9.91 (s, 8H, β-H). UV–vis [$(CH_3)_2CO$] λ_{max}: 425 nm (ε 345,800), 556 (12,500), 595 (6200).

5.6. *meso*-Tetra[bis-3,5-(1-methyl-*nido*-carboranyl)methylphenyl]porphyrin tetrasodium salt (5)

To a solution of Zn(II)-porphyrin **4** (0.016 g, 0.007 mmol) in 1 mL of methanol were added 2 mL of TFA and one drop of sulfuric acid, and the final mixture was stirred for 30 min at room temperature. The reaction mixture was concentrated under vacuum, diluted with methanol and neutralized by dropwise addition of triethylamine. The solvent was completely removed under vacuum, the residue redissolved in a 40% aqueous acetone solution and slowly passed through a Dowex 50WX2-100 resin in the sodium form. The porphyrin fraction was collected, concentrated under vacuum, redissolved in a 70% aqueous acetone solution and again passed through the ion-exchange resin. The solvent was removed under vacuum to afford 0.015 g (96%) of the title porphyrin, mp > 300 °C. ^{1}H NMR (acetone-d_6) δ ppm: −2.59 (s, 2H, NH), −2.33 (br, 8H, BH), 1.5–3.0 (br, 72H, BH), 2.05 (s, 24H, CH_3), 3.45 (s, 16H, CH_2), 7.86 (m, 4H), 8.07 (m, 8H), 9.12 (m, 8H, β-H). UV–vis [$(CH_3)_2CO$] λ_{max}: 420 nm (ε 327,700), 516 (13,600), 552 (9900), 592 (5700), 647 (5700).

6. Molecular structure

The crystal structure of a cyclohexane/dichloromethane solvate of porphyrin **2** was determined, using data collected at $T = 105$ K to $\theta = 22.5°$ with MoKα radiation on a Nonius KappaCCD diffractometer. Crystal data: $C_{76}H_{142}B_{80}N_4{\cdot}5C_6H_{12}{\cdot}2CH_2Cl_2$, triclinic space group $P\bar{1}$, $a = 11.389(8)$, $b = 18.753(13)$, $c = 19.182(17)$ Å, $\alpha = 88.43(3)$, $\beta = 73.31(3)$, $\gamma = 79.00(7)°$, $V = 3851(5)$ Å^3, $Z = 1$, $R = 0.104$ ($F^2 > 2\sigma$), $Rw = 0.275$ (all F^2) for 8372 unique data and 894 refined parameters. An electron density peak at the porphyrin center likely represents partial occupancy by a metal complex, the identity of which remains uncertain. It was modeled as substitution by 8% Cu. Crystallographic data (excluding structure factors) for the structure in this paper have been deposited with the Cambridge Crystallographic Data Centre as supplementary publication no. CCDC 251020. Copies of the data can be obtained, free of charge, on application to CCDC, 12 Union Road, Cambridge, CB2 1EZ, UK, (fax: +44-(0)1223-336033 or e-mail: deposit@ccdc.cam.ac.uk).

7. Cell culture

Hamster lung fibroblast V79 cells and human glioblastoma T98G cells were obtained from ATCC. The V79 cells were maintained in Dulbecco's Modified Eagle Medium (DMEM) supplemented with 10% fetal bovine serum (FBS) and the T98G cells were maintained in 50% of α-MEM/advanced MEM supplemented with 10% FBS. Phosphate buffered saline (PBS), FBS, and trypsin were purchased from Gibco, the Giemsa solution from Fluka, Cyquant reagent from Molecular Probes, triton X-100 from Calbiochem and lysoSensor from Molecular Probes. The microscopy was performed on a Zeiss Axiovert 200M inverted fluorescent microscope fitted with a standard Texas Red and FITC filter sets (Chroma Technology Corp.). Compounds **4** and **5** were dissolved in DMSO prior to being diluted into medium; the final DMSO concentration never exceeded 1%. All medium solutions were filter sterilized (22 μm pore size) prior to use.

7.1. Dark cytotoxicity

Chinese hamster V79 cells were sub-cultured and incubated for 24 h with porphyrin **5** solutions of 0 (standards), 100, 150, 200, and 250 μM concentrations, as we have previously reported.[19] After incubation, the cells were washed with PBS and harvested by adding 0.25% trypsine in PBS solution for 10 min at 37 °C. DMEM was then added, the cells counted and trans-

ferred (100, 300, or 1000 cells for each porphyrin concentration) to 10 cm Petri dishes containing 10 mL DMEM. The clones were allowed to grow for 6–7 days, then washed with PBS, fixed with methanol for 10 min and stained with Giemsa solution for 40 min. After removal of the Giemsa solution, the clones were washed with ethanol/water (7:3) and counted. Each determination was performed in triplicate for each porphyrin concentration.

7.2. Concentration-dependent cellular uptake

Human T98G cells were cultured on a 96-well plate at the concentration of 20,000 cells/100 μL in each well. A 200 μM solution of H_2OCP (**5**) in DMSO was prepared, filter sterilized, and two-fold dilution series were accomplished to afford porphyrin concentrations of 200, 100, 50, 25, 12.5, 6.25, 3.125, and 0 μM. After 3 h incubation time the cells were washed with PBS, and 100 μL of 0.25% triton X-100 in PBS was added to each well. To obtain a standard graph for H_2OCP (**5**) a 20 μM solution of H_2OCP (**5**) in 0.25% triton X-100 was prepared and used to make a dilution series of 10, 5, 2.5, 1.25, 0.625, 0.3125, and 0 μM. The porphyrin fluorescence was measured on a FLUOstar plate reader using 570 nm excitation and 650 nm emission filters. The standard curve for different cell numbers was obtained by placing 100,000, 80,000, 60,000, 40,000, 20,000, 10,000, and 0 cells in the wells followed by incubation for 3 h. The cell numbers were determined by adding 100 μL/well of a 2X stock solution of Cyquant reagent in PBS. The plate was read on the FLUOstar plate reader using 480 nm excitation and 520 nm emission filters.

7.3. Time-dependent cellular uptake

Human T98G cells were subcultured as described above. A stock solution of porphyrin **5** in DMSO was diluted with α-MEM/advance medium to make a 10 μM solution, which was filter sterilized. After incubation for 48 h the 10 μM porphyrin solution was added and the cells incubated for 24, 8, 4, 2, 1, and 0 h periods. The cells were washed with PBS and 100 μL of 0.25% triton X-100 in PBS was added to each well. The standard graph for H_2OCP (**5**), the porphyrin fluorescence and cell numbers were determined as described above. The same procedure was followed for the time-dependent uptake of porphyrins **4** and **6**.

7.4. Intracellular localization

T98G cells were grown in a Lab-Tek II chamber coverglass system with the same culture medium as described above. H_2OCP (**5**) was added to reach a final concentration of 50 μM. The cells were incubated in the dark for 4 h, then washed with drug-free medium three times to remove unbound porphyrin. Fresh medium containing 50 mM HEPES pH 7.2 was added to cells and these examined immediately by fluorescence microscopy. Co-localization experiments were performed using 100 nM concentration of lysoSensor. The cells were incubated with porphyrin as described above, and the lysoSensor was added 30 min before completion of the incubation time.

Acknowledgements

The research described was supported by the National Institutes of Health, grant number 1R01 CA098902.

References and notes

1. Nakagawa, Y.; Pooh, K.; Kobayashi, T.; Kageji, T.; Uyama, S.; Matsumura, A.; Kumada, H. *J. Neuro-Oncol.* **2003**, *62*, 87–99.
2. Busse, P. M.; Harling, O. K.; Palmer, M. R.; Kiger, W. S., III; Kaplan, J.; Kaplan, I.; Chuang, C. F.; Goorley, J. T.; Riley, K. J.; Newton, T. H.; Santa Cruz, G. A.; Lu, X.-Q.; Zamenhof, R. G. *J. Neuro-Oncol.* **2003**, *62*, 111–121.
3. Joensuu, H.; Kankaanranta, L.; Seppälä, T.; Auterinen, I.; Kallio, M.; Kulvik, M.; Laakso, J.; Vähätalo, J.; Kortesniemi, M.; Kotiluoto, P.; Serén, T.; Karila, J.; Brander, A.; Järviluoma, E.; Ryynänen, P.; Paetau, A.; Ruokonen, I.; Minn, H.; Tenhunen, M.; Jääskeläinen, J.; Färkkilä, M.; Savolainen, S. *J. Neuro-Oncol.* **2003**, *62*, 123–134.
4. Capala, J.; Stenstam, B. H.; Sköld, K.; af Rosenschöld, P. M.; Giusti, V.; Persson, C.; Wallin, E.; Brun, A.; Franzen, L.; Carlsson, J.; Salford, L.; Ceberg, C.; Persson, B.; Pellettieri, L.; Henriksson, R. *J. Neuro-Oncol.* **2003**, *62*, 135–144.
5. Barth, R. F.; Soloway, A. H.; Fairchild, R. G.; Brugger, R. M. *Cancer* **1992**, *70*, 2995–3007.
6. Barth, R. F.; Soloway, A. H.; Goodman, J. H.; Gahbauer, R. A.; Gupta, N.; Blue, T. E.; Yang, W.; Tjarks, W. *Neurosurgery* **1999**, *44*, 433–451.
7. Fairchild, R. G.; Bond, V. P. *Int. J. Rad. Oncol. Biol. Phys.* **1985**, *11*, 831–840.
8. Gabel, D.; Foster, S.; Fairchild, R. G. *Radiat. Res.* **1987**, *111*, 14–25.
9. Soloway, A. H.; Tjarks, W.; Barnum, B. A.; Rong, F. G.; Barth, R. F.; Codogni, I. M.; Wilson, J. G. *Chem. Rev.* **1998**, *98*, 1515–1562.
10. Vicente, M. G. H. *Curr. Med. Chem., Anti-Cancer Agents* **2001**, *1*, 175–194.
11. Bregadze, V. I.; Sivaev, I. B.; Gabel, D.; Wöhrle, D. *J. Porphyrins Phthalocyanines* **2001**, *5*, 767–781.
12. Ceberg, C. P.; Brun, A.; Kahl, S. B.; Koo, M. S.; Persson, B. R. R.; Salford, L. G. *J. Neurosurg.* **1995**, *83*, 86–92.
13. Miura, M.; Micca, P. L.; Fisher, C. D.; Gordon, C. R.; Heinrichs, J. C.; Slatkin, D. N. *Br. J. Radiol.* **1998**, *71*, 773–781.
14. Vicente, M. G. H.; Wickramasinghe, A.; Nurco, D. J.; Wang, H. J. H.; Nawrocky, M. M.; Makar, M. S.; Miura, M. *Bioorg. Med. Chem.* **2003**, *11*, 3101–3108.
15. Lee, J.; Park, Y. S.; Kim, Y.; Kang, H. C. *Bull. Korean Chem. Soc.* **1999**, *20*, 1371–1372.
16. Vicente, M. G. H.; Edwards, B. F.; Shetty, S. J.; Hou, Y.; Boggan, J. E. *Bioorg. Med. Chem.* **2002**, *10*, 481–492.
17. Vicente, M. G. H.; Shetty, S.; Wickramasinghe, A.; Smith, K. M. *Tetrahedron Lett.* **2000**, *41*, 7623–7627.
18. Lauceri, R.; Purrello, R.; Shetty, S. J.; Vicente, M. G. H. *J. Am. Chem. Soc.* **2001**, *123*, 5835–5836.
19. Vicente, M. G. H.; Nurco, D. J.; Shetty, S. J.; Osterloh, J.; Ventre, E.; Hegde, V.; Deutsch, W. A. *J. Photochem. Photobiol. B: Biol.* **2002**, *68*, 123–132.
20. Vicente, M. G. H.; Gottumukkala, V.; Wickramasinghe, A.; Anikovsky, M.; Rodgers, M. A. J. *Proc. SPIE* **2004**, *5315*, 33–40.
21. Vicente, M. G. H.; Nurco, D. J.; Shetty, S. J.; Medforth, C. J.; Smith, K. M. *Chem. Commun.* **2001**, 483–484.

22. Nurco, D. J. University of California Davis, unpublished results.
23. Woodburn, K.; Phadke, A. S.; Morgan, A. R. *Bioorg. Med. Chem. Lett.* **1993**, *3*, 2017–2022.
24. Hill, J. S.; Kahl, S. B.; Stylli, S. S.; Nakamura, Y.; Koo, M.-S.; Kaye, A. H. *Proc. Natl. Acad. Sci. U.S.A.* **1995**, *92*, 12126–12130.
25. Matsumura, A.; Shibata, Y.; Yamamoto, T.; Yoshida, F.; Isobe, T.; Nakai, K.; Hayakawa, Y.; Kiriya, M.; Shimojo, N.; Ono, K.; Sakata, I.; Nakajima, S.; Okumura, M.; Nose, T. *Cancer Lett.* **1999**, *141*, 203–209.
26. Bobadova-Parvanova, P.; Oku, Y.; Wickramasinghe, A.; Hall, R. W.; Vicente, M. G. H. *J. Porphyrins Phthalocyanines* **2004**, *8*, 996–1006.
27. Osterloh, J.; Vicente, M. G. H. *J. Porphyrins Phthalocyanines* **2002**, *6*, 305–324.
28. Nguyen, T.; Brownell, G. L.; Holden, S. A.; Kahl, S.; Miura, M.; Teicher, B. A. *Radiat. Res.* **1993**, *133*, 33–40.
29. Callahan, D. E.; Forte, T. M.; Afzal, S. M. J.; Deen, D. F.; Kahl, S. B.; Bjornstad, K. A.; Bauer, W. F.; Blakely, E. A. *Int. J. Rad. Oncol. Biol. Phys.* **1999**, *45*, 761–771.